

Mechanical Unfolding of Ubiquitin Molecules

Marek Cieplak¹ and Piotr E. Marszalek²

¹ *Institute of Physics, Polish Academy of Sciences, Al. Lotników 32/46, 02-668 Warsaw, Poland*

² *Department of Mechanical Engineering and Materials Science, Duke University, 144 Hudson Hall,
Durham, NC 27708-0300, USA*

Keywords: mechanical stretching of proteins; Go model; molecular dynamics; ubiquitin; titin; AFM

PACS numbers: 82.37.Rs, 87.14.Ee, 87.15.-v

Abstract

Mechanical stretching of ubiquitin and of its several repeats are studied through molecular dynamics simulations. A Go-like model with a realistic contact map and with Lennard-Jones contact interactions is used. The model qualitatively reproduces the experimentally observed differences between force-extension patterns obtained on polyubiquitins stretched by various linkages. The terminal-to-terminal stretching of polyubiquitin results in peak forces similar to those measured for titin-based polyproteins and of a magnitude that matches measurements. Consistent with the experimental measurements, the simulated peak forces depend on the pulling speed logarithmically when thermal fluctuations are explicitly introduced. These results validate the application of topology-based models in the study of the mechanical stretching of proteins.

INTRODUCTION

Mechanical stretching of proteins is a natural phenomenon that takes place *in vivo* in various cellular processes such as protein degradation by ATP-dependent proteases and translocation through membranes¹⁻⁴, cell locomotion, replication, and many other⁵. It can also be induced experimentally by means of an atomic force microscope (AFM), optical and magnetic tweezers and other. The mechanical manipulation of individual proteins is rapidly becoming an important approach to probe their structural and elastic properties (see for instance⁶). Large proteins that play important mechanical roles such as muscle titin had already been extensively studied experimentally⁷⁻¹⁶ and these investigations were soon followed by theoretical studies of single¹⁷⁻²⁰ and multiple²¹⁻²³ domains of titin. In this paper, we consider stretching of ubiquitin. Ubiquitin is an α/β protein which varies little across species in eucariotic cells. The human ubiquitin is a small protein composed of 76 amino acids^{24,25} which is able to naturally form polyproteins that are connected either through their N-C termini or through the C terminus and one of the four lysine residues (K63,K48,K29,K11). Polyubiquitins tag other proteins and in the linkage-dependent manner destine them e.g. for degradation by proteasomes²⁶⁻²⁸ or direct them for transport through cell membranes²⁹.

AFM studies of ubiquitin exploited its unusual ability to form homopolyproteins which can transmit the stretching forces to various segments of the monomer via different linkages (different attachment points). They focused on measuring the mechanical stability of ubiquitin monomers under various stretching conditions^{30,31} and demonstrated the existence of well defined stages in ubiquitin folding³². The stretching studies³⁰ have indicated that elastic properties of these polyproteins are linkage dependent. Two specific cases have been considered: terminal-to-terminal (or the N-C polyubiquitin) and Lys48-to-terminal C (or the Lys48-C polyubiquitin). The former linkage yields titin-like sawtooth-like pattern of unfolding forces of about 200 pN separated by 24 nm, the length corresponding to the increase in the polyubiquitin contour length upon unfolding of one ubiquitin monomer³⁰. The Lys48-C polyubiquitin, on the other hand, yields a distinct saw-tooth

pattern with unfolding forces of about 85 pN separated by only 7.8 nm, the contour length increment that is consistent with the unfolding of a portion of one ubiquitin monomer that encompasses Lys48 and C terminus. Steered molecular dynamics simulations of ubiquitin monomers immersed in molecular water and stretched by these two types of linkages qualitatively reproduced the differences between their mechanical unfolding patterns³⁰. However, the unfolding forces determined by these simulations are an order of magnitude greater than measured by the AFM. This is because the extension rates in computer simulations are 6-7 orders of magnitude faster than the experimental rates. Because the experimentally found dependence of the unfolding forces on the pulling speed is logarithmic³¹ the bridging of the gap between the steered molecular dynamics modeling and the experiment is rather unlikely (see also²³). The all-atom-based Monte Carlo determination of the free energy of ubiquitin monomers immersed in a continuum solvent³³ does generate the mean forces, at a given extension, which are consistent with the AFM measurements for both types of ubiquitin chains. However, the free-energy-based approach does not yield relationships between force, F , and extension, L , or force and tip displacement, d , which capture all the details of the unfolding events. The distinction between L and d is that, under the conditions of constant pulling speed, d increases linearly with time whereas L varies in time in a non-uniform manner that reflect the instantaneous tension.

The purpose of this paper is to demonstrate that simple coarse-grained and topology-based dynamical models reproduce the main features of the experimental force–extension curves of ubiquitin pulled at constant speed. We also show that the $F - L$ and $F - d$ relationships obtained on ubiquitins are linkage-dependent. In particular, the saw-tooth patterns generated by N-C-linked polyubiquitins are similar to those for titin by the same kind of a model. In addition, we show that the details of the force patterns depend on the number of monomers in the chain and that they display a strong sensitivity to the temperature. The model also correctly reproduces the dependence of the unfolding force on the stretching speed. In addition to modeling the mechanics of naturally occurring N-C and Lys48-C linked polyubiquitins, which have been investigated before using the steered molecular dynamics approach, we also consider the effects of transmitting the force to

various parts of the protein by exploiting other natural and hypothetical linkages. We find that ubiquitin offers a particularly large resistance to unfolding when the stretching force is transmitted by the N-terminus and glycine 40. It should be noted that a recent Go-like modeling of ubiquitin³⁴ has been used to monitor refolding after stretching of polyubiquitin at constant force³².

MODEL AND METHOD

To model the mechanical properties of ubiquitin (PDB code 1ubq³⁵) we use the Go-like model^{36,37} with the ground state corresponding to the conformation of the native state. This conformation is determined experimentally at room temperature. The details of our approach can be found in references^{38–40} with the updates as detailed in references⁴¹ and²¹. Briefly, the native contacts between amino acids are determined pair by pair and by checking for overlapping of the atoms, following reference⁴². The native contacts are described by the Lennard-Jones potentials:

$$V_{ij} = 4\epsilon \left[\left(\frac{\sigma_{ij}}{r_{ij}} \right)^{12} - \left(\frac{\sigma_{ij}}{r_{ij}} \right)^6 \right]. \quad (1)$$

The length parameters, σ_{ij} , in these potentials are selected so that the minima of the potentials agree with the experimentally determined distance between the C^α atoms at contact. The non-native contacts correspond to a repulsive core of $\sigma = 5\text{\AA}$. The energy parameter, ϵ , is taken to be uniform and its value should be in the range 800-2300 K since it corresponds to an effective average of all non-covalent interactions in proteins. We take 900 K to be a representative value of ϵ . This choice corresponds to a lower energy scale than of order 2000 K that typically characterizes hydrogen bonds. However, the Lennard-Jones potentials are broader in spatial extension than those found in more realistically described interactions. The energetic effect of a potential is related to an integral over the potential. Thus making the potential more extended requires reducing its amplitude. Our previous simulations of folding^{41,21} point to fast and optimal folding at the dimensionless temperature $\tilde{T} = k_B T / \epsilon$ of order 0.3 which corresponds to room temperature if ϵ is around 900 K. (k_B is the Boltzmann constant and T is temperature). In addition, the

simulated mechanical stretching curves also acquire similarity to experiments at $\tilde{T}=0.3^{21,22}$. With $\epsilon = 900$ K, the unit of force used in this paper, $\epsilon/\text{\AA}$ corresponds to 120 pN. This choice also yields the correct magnitude of the force peak in titin at room temperature²¹.

In reference²², we have explored a possibility of enhancing, by a factor of two, the contacts between hydrophobic amino acids. This correction did not significantly change the force-displacement curves other than altering the overall energy scale. The tethering potential between the consecutive C^α atoms that binds them at the peptide bond length is purely harmonic with a strong spring constant of $100 \epsilon/\text{\AA}^2$. The model also contains a four-body chirality term that favors the native sense of chirality. This term is taken in the form as presented in ref.⁴³. Its effects on protein stretching are minimal, but become significant during protein folding. Tandem arrangements of several domains are constructed by repeating 1ubq domain in series with one extra peptide link between the designated terminal residues. If necessary, a rotation⁵ is implemented to avoid native steric clashes. In our stretching simulations, both ends of the protein are attached to harmonic springs of spring constant $k=0.12 \epsilon/\text{\AA}^2$ which is close to the values corresponding to the elasticity of experimental cantilevers. The free end of one of the two springs is constrained while the free end of the second spring is pulled at constant speed, v_p , along the initial end-to-end position vector. Our typical v_p is $0.005 \text{\AA}/\tau$ except in the simulations which were aimed at investigating the effect of the pulling speed. $\tau = \sqrt{m\sigma^2/\epsilon} \approx 3\text{ps}$ is the characteristic time for the Lennard-Jones potentials, where $\sigma = 5\text{\AA}$ is a typical value of σ_{ij} and m is the average mass of the amino acids. The thermal fluctuations away from the native state are introduced by means of the Langevin noise⁴⁴, i.e. by random Gaussian forces together with a velocity dependent damping. This noise provides thermostating and generally mimicks the random effects of the solvent.

The ground state of our model corresponds to the native state of the protein at room temperature. Thus the meaning of the temperature in any Go-like model is fairly qualitative since real proteins undergo structural fluctuations already at room temperature. The temperature T should then

be understood as a control parameter that allows the modeling of protein fluctuations including those present under room temperature. In order to register thermal effects on the force-extension relationship it is thus necessary to average the evolution over a time interval. We demonstrate that sufficient averaging and sensitivity to persistent features is achieved by choosing the observation resolution that corresponds to a pulling distance of 0.5 Å.

An equation of motion for each C^α reads

$$m\ddot{\mathbf{r}} = -\gamma\dot{\mathbf{r}} + F_c + \Gamma . \quad (2)$$

F_c is the net force due to the molecular potentials. The damping constant γ is taken to be equal to $2m/\tau$ and the dispersion of the random forces is equal to $\sqrt{2\gamma k_B T}$. This choice of γ corresponds to a situation in which the inertial effects are negligible⁴¹ but the damping action is not yet as strong as in water. Increasing γ tenfold results in a tenfold increase in the time scales bringing the typical value of v_p within two orders of magnitude of the experimental pulling speeds^{41,21}. The equations of motion are solved by a fifth order predictor-corrector scheme.

RESULTS AND DISCUSSION

Stretching of one ubiquitin

The backbone representation of 1ubq is shown in Figure 1 where possible linkage points are marked in black. The native ubiquitin contains one α -helix (amino acids 23-34), two 310-helices (38-40 and 57-59) and several β -strands (2-16, 41-49, and 66-71). The β -content of 31.6% is about twice as high as the α -content. Ubiquitin structure contrasts the structure of the I27 domain of titin that does not contain any helical fragments.

We first consider stretching of a single ubiquitin unit. Figure 2 shows snapshots of an ubiquitin monomer stretched by external forces attached to the module at the indicated residues. These

simulations correspond to $\tilde{T} = 0$ and the snapshots were captured at an instant when the simulated AFM tip moved by 100 Å. The N-terminal is shown at the left side of each panel. In each of these three cases, the α -helix remains unraveled. When the pulling force is attached to residues 1 and 76 or to 1 and 48, the vicinity of the C-terminal extends. This is not the case when the stretching forces are attached to residues 1 and 40. In this last case, the C-terminal is still attached to the folded part of the protein. Figure 3 compares the examples of the force–displacement curves for Iubq obtained at \tilde{T} of 0 and 0.3. The latter \tilde{T} corresponds to the thermal fluctuations experienced by the protein near room temperature²¹. Three cases of force attachment are considered in Figure 3. N-C (the top panel) and Lys48-C (the middle panel) represent naturally occurring polyubiquitin linkages. The third linkage considered, N-Lys48 (bottom panel) does not occur naturally. However, it is informative to focus also on this portion of the protein because it experiences significant stretching forces when it is pulled by the N and C termini. In each of these three cases, the thermal fluctuations facilitate the stretching, decrease the force peaks and shift them towards shorter extensions. For a general discussion of the thermal effects in stretching see reference²¹ and⁴⁵ and the experimental results of Janoviak et al.⁴⁶.

The closer comparison of the traces obtained at $\tilde{T} = 0.3$ and $\tilde{T}=0$ suggests, however, that the former are just somewhat rescaled versions of the latter. Thus, when analyzing the role of various linkages in the mechanics of polyubiquitins, we focus on the subset of the force–displacement curves obtained at $\tilde{T} = 0$. It is interesting that these curves differ greatly among themselves. Stretching by the N and C termini generates the greatest peak force – of about $4\epsilon/\text{Å}$ at $\tilde{T} = 0$. This value is close to that obtained for a single I27 domain of titin when stretched by the N and C termini within the same model²¹. In spite of the similar mechanical stability of ubiquitin and I27 domain of titin, their force–displacement curves differ in many details. For example, the ubiquitin trace displays three well defined major force peaks compared to two force peaks of I27 domain. In addition, the ubiquitin force peaks are broader. On raising the ubiquitin temperature to $\tilde{T} = 0.3$, the second and third major peaks in its force–displacement relationship appear closer to each other and it is more difficult to identify them as separate peaks.

When the stretching forces are attached to Lys48 and the C-terminus, the force–displacement curve obtained at $\tilde{T} = 0$ displays two major force peaks of about $2.5\epsilon/\text{\AA}$ and $1.8\epsilon/\text{\AA}$ at $\tilde{T} = 0$. Because, in this case, only 29 residues between Lys48 and the C-terminus are pulled, the maximum extension corresponds to approximately a half of the extension registered when the complete domain is unraveled. When the stretching is accomplished by forces attached to the N-terminus and Lys48, the force–displacement curve displays a new and distinct pattern. The first major peak is now much broader, with a maximum force of about $3\epsilon/\text{\AA}$ at $\tilde{T} = 0$ and it is composed of five easily identifiable peaks ranging in force between 2.3 and $3\epsilon/\text{\AA}$. It is interesting to note that the force-displacement profile obtained upon stretching ubiquitin by its N-C termini is not a simple piece-wise superposition of the patterns obtained when stretching the protein by its N-terminus and Lys48 and by Lys48 and the C-terminus. This suggests that the stretching by the N and C termini involves breaking of the contacts that had been formed between the segments to the left and to the right of Lys48.

Figure 4 illustrates the distinction between the $F - d$ and $F - L$ patterns. Consider first the pulling by the terminal points (the top panel of Figure 4). As the AFM tip moves uniformly, the end-to-end distance between the termini may vary in sudden jumps, especially just after crossing major force peaks. Thus when plotting F vs. L one gets a pattern which has a different visual appearance from that corresponding to the $F - d$ pattern (the top panel of Figure 3). When the pulling springs are attached at non-terminal points, as in the remaining panels of figure 4, the end-to-end distance is replaced by the distance between the point of attachment – L .

Figure 5 further explores the dependence of the force–displacement curve on the attachment of the force to one of the remaining lysine residues and also includes a special case when the fragment between the N-terminus and glycine 40 is subjected to stretching forces. It is interesting that the tallest force peak is generated when ubiquitin is stretched by the N-terminus and Gln40 suggesting that forces transmitted by this residue need to break the most resistant bonds within the

protein.

Breaking the contacts between amino acids

We now follow the contacts between various residues during the stretch. We investigate the average tip displacement distance, d_u , at which these contacts break definitely as a function of the contact order. The contact order is defined as the sequential distance, $|j - i|$, between a pair of amino acids i and j that make a contact in the native state. For a contact to hold we require that the $C^\alpha-C^\alpha$ distance does not exceed $1.5\sigma_{ij}$. Figure 6 shows the rupture distances in the initial stages of stretching at $\tilde{T}=0$. The symbols are defined in the caption. The stretching by the N and C-termini causes the contact between residues 40 and 73 to yield first. Residue 40 belongs to one of the 310 helices and residue 73 is in the vicinity of the C-terminal. The next stage involves rupturing of the β sheet formed by two strands: 1-7 and 12-17. The stretching by residues 1 and 40 starts with the rupture of the same β sheet so the initial stages of these two types of stretching are indeed quite similar. The stretching by residues 1 and 48, on the other hand, starts around the 41-49 strand whereas the stretching by residues 48 and 76 first affects the interaction between two strands: 41-49 and 65-72. The buildup of the maximum force in the N-C case involves the helix and the three β strands: contacts between 1-7, 12-17 and 65-72; and between 41-49 and 65-72. These events need to be further validated.

We now consider the dependence of the maximum force, F_{max} , on the pulling speed. We consider the pulling by the N and C termini and by Lys48 and the C-terminus, as shown in Figure 7. The values of v_p range from 0.00005 to 0.001 $\text{\AA}/\tau$. The smallest value of v_p corresponds to the highest speed used experimentally. The data points obtained for $\tilde{T}=0$ show an imperceptible dependence on v_p except around the fastest speeds used in the simulations modeling the stretching of ubiquitin by lysine 48 and the C-terminus. At finite temperatures this dependence is logarithmic (the average was done over several trajectories). The slope of the lines representing this dependence seems to be affected more by the points of the force attachment (it is the greatest in the N-C case) rather than by \tilde{T} .

Stretching of five ubiquitins connected in tandem

Figure 8 shows the force-displacement relationships obtained for two ubiquitin polyproteins composed of five tandem repeats connected in series using the linkages between the N- and C-termini (top panel) and linkages between Lys48 and the C-terminus (bottom panel). The force-extension profiles obtained for $\tilde{T} = 0$ are nearly periodic repeats of a single "wavelet". Only the first period of the force-displacement curve displays a somewhat distinct force peak pattern. This suggests that the low temperature unfolding events of individual ubiquitins are not correlated, which is similar to what is observed for titin. This behavior is due to the large magnitude of the peak force. This phenomenon is less obvious when polyubiquitin is stretched by Lys48 and the C-terminus. Figure 9 replots the data of Figure 8 so that F is shown against the extension. It is seen that in the multiple-domain case the differences between the $F - d$ and $F - L$ patterns are much less pronounced. It should be noted that the $F - L$ patterns start at a finite extension whereas the $F - d$ patterns start at 0.

Figure 10 shows two snapshots of polyubiquitin composed of five repeats that were stretched at $\tilde{T} = 0$ to the tip displacement of $d=250 \text{ \AA}$. When the stretching occurs by the N and C-termini, the first module is nearly unfolded at this stage. When the stretching occurs by the Lys48 and the C-terminus, the part of the first module which encompasses residues 48 through 76 is nearly fully stretched (the 1-Lys48 fragment is dangling) and all other units are partially unfolded, with the first unit being stretched the most. The further stretching proceeds with no correlation between the behavior of individual units, for both types of the linkages. On increasing the temperature, the parallel events gain in importance⁴⁵ and the traces shed peaks. Except for the first 'period' which has two distinct peaks at $\tilde{T} = 0.3$, the remaining periods have essentially no peaks other than the major one that was observed for a single ubiquitin. It is significant that the patterns corresponding to $\tilde{T} = 0.3$ are qualitatively similar to the force-extension curves measured in the AFM experiments³⁰, correctly reproduce the difference between both types of linkages, and yield peak forces of the correct order of magnitude. The logarithmic dependence on the pulling speed ob-

tained in the simulations of one ubiquitin is consistent with the experimental dependence observed for polyubiquitin^{30,31}.

We conclude that a simple coarse grained Go-like model captures the essential features of the experimental results obtained on ubiquitin polyproteins. This encourages its application to studying the mechanical properties of other proteins.

ACKNOWLEDGMENTS

This work was funded by the Ministry of Science in Poland (grant 2P03B 032 25).

REFERENCES

- ¹ S. Huang, K. S. Ratliff and A. Matouschek, *Nature Struct. Biol.* **9** 301 (2002).
- ² A. Matouschek, *Curr. Op. Struct. Biol.* **13** 98 (2003).
- ³ A. Matouschek and C. Bustamante, *Nature Struct. Biol.* **10** 674 (2003).
- ⁴ S. Prakash and A. Matouschek, *Trends Bioch. Sci.* **29** 593 (2004).
- ⁵ C. Bustamante, Y. R. Chemla, N. R. Forde, and D. Izhaky, *Annu. Rev. Biochem.* **73** 705 (2004).
- ⁶ M. Carrion-Vazquez, A. F. Oberhauser, T. E. Fisher, P. E. Marszalek, H. Li, and J. M. Fernandez, *Prog. Biophys. & Mol. Biol.* **74** 63091 (2000).
- ⁷ H. P. Erickson, *Science* **276** 1090 (1997).
- ⁸ W. A. Linke, M. Ivemeyer, N. Olivieri, B. Kolmerer, J. C. Ruegg JC, and S. Labeit, *J. Mol. Biol.* **261** 62 (1996).
- ⁹ L. Tskhovrebova, K. Trinick, J. A. Sleep, M. Simmons, *Nature* **387** 308 (1997).
- ¹⁰ M. S. Z. Kellermayer, S. B. Smith, H. L. Granzier, and C. Bustamante, *Science* **276** 1112 (1997).
- ¹¹ M. Rief, M. Gautel, F. Oesterhelt, J. M. Fernandez JM, and H. E. Gaub, *Science* **276** 1109 (1997).
- ¹² P. E. Marszalek, H. Lu, H. B. Li, M. Carrion-Vazquez, A. F. Oberhauser, K. Schulten, and J. M. Fernandez, *Nature* **402** 100 (1999).
- ¹³ M. Carrion-Vasquez, A. F. Oberhauser, S. B. Fowler, P. E. Marszalek, S. E. Broedel, J. Clarke, and J. M. Fernandez, *Proc. Natl. Acad. Sci. (USA)* **96** 3694 (1999).
- ¹⁴ A. F. Oberhauser, P. K. Hansma, M. Carrion-Vazquez, and J. M. Fernandez, *Proc. Natl. Acad. Sci. (USA)* **98** 468 (2001).
- ¹⁵ A. F. Oberhauser, P. E. Marszalek, M. Carrion-Vazquez, and J. M. Fernandez, *Nat. Struct. Biol.* **6** 1025 (1999)

- ¹⁶ B. L. Smith, T. E. Schaeffer, M. Viani, J. B. Thompson, N. A. Frederic, J. Kindt, A. Belcher, G. D. Stucky, D. E. Morse, and P. K. Hansma, *Nature* **399** 761 (1999).
- ¹⁷ H. Lu, B. Isralewitz, A. Krammer, V. Vogel, and K. Schulten, *Biophys. J.* **75** 662 (1998).
- ¹⁸ H. Lu and K. Schulten, *Chem. Phys.* **247** 141 (1999).
- ¹⁹ E. Paci and M. Karplus, *Proc. Natl. Acad. Sci. (USA)* **97** 6521 (2000).
- ²⁰ M. Cieplak, T. X. Hoang and M. O. Robbins, *Proteins: Struct. Funct. Bio.* **49** 114 (2002).
- ²¹ M. Cieplak, T. X. Hoang and M. O. Robbins, *Proteins: Struct. Funct. Bio.* **56** 285 (2004).
- ²² M. Cieplak, A. Pastore and T. X. Hoang, *J. Chem. Phys.* **122** 054906 (2004).
- ²³ M. Cieplak, *Physica A* **352** 28 (2004).
- ²⁴ S. Vijay-Kumar, C. E. Bugg and W. J. Cook, *J. Mol. Biol.* **194** 531 (1987).
- ²⁵ K. Lindorff-Larsen, R. B. Best, M. A. DePristo, C. M. Dobson, and M. Vendruscolo, *Nature* **433** 128 (2005).
- ²⁶ C. M. Pickart, *Annu. Rev. Biochem.* **70** 503 (2001).
- ²⁷ M. Hochstrasser and J. Wang, *Nat. Struct. Biol.* **8** 294 (2001).
- ²⁸ A. M. Weissman, *Nat. Rev. Mol. Cell. Biol.* **2** 169 (2001).
- ²⁹ L. Hicke and R. Dunn, *Annu. Rev. Cell. Dev. Biol.* **19** 141 (2003).
- ³⁰ M. Carrion-Vazquez, H. Li, H. Lu, P. E. Marszalek, A. F. Oberhauser, and J. M. Fernandez, *Nat. Struct. Biol.* **10** 738 (2003).
- ³¹ C-L. Chyan, F-C. Lin, H. Peng, J-M. Yuan, C-H. Chang, S-H. Lin, and G. Yang, *Bioph. J.* **87** 3995 (2004).
- ³² J. M. Fernandez and H. Li, *Science* **303** 1674 (2004).
- ³³ P-C. Li and D. E. Makarov, *J. Chem. Phys.* **121** 4826 (2004).

- ³⁴ R. B. Best and G. Hummer, *Science* **308** 498b (2005).
- ³⁵ F. C. Bernstein, T. F. Koetzle, G. J. B. Williams, E. F. Meyer Jr., M. D. Brice, J. R. Rodgers, O. Kennard, T. Shimanouchi, and M. Tasumi M, *J. Mol. Biol.* **112** 535 (1997).
- ³⁶ H. Abe and N. Go, *Biopolymers* **20** 1013 (1981).
- ³⁷ S. Takada, *Proc. Natl. Acad. Sci. (USA)* **96** 11698 (1999).
- ³⁸ T. X. Hoang and M. Cieplak, *J. Chem. Phys.* **112** 6851 (2000).
- ³⁹ T. X. Hoang and M. Cieplak, *J. Chem. Phys.* **113** 8319 (2001).
- ⁴⁰ M. Cieplak and T. X. Hoang, *Proteins: Struct. Funct. Bio.* **44** 20 (2001).
- ⁴¹ M. Cieplak and T. X. Hoang, *Biophysical J.* **84** 475 (2003).
- ⁴² J. Tsai, R. Taylor, C. Chothia, and M. Gerstein, *J. Mol. Biol.* **290** 253 (1999).
- ⁴³ J. I. Kwiecinska and M. Cieplak, *J. Phys: Cond. Mat.* **17** S1565 (2005).
- ⁴⁴ G. S. Grest and K. Kremer, *Phys. Rev. A* **33** 3628 (1986).
- ⁴⁵ M. Cieplak, T. X. Hoang and M. O. Robbins, *Phys. Rev. E* **69** 011912 (2004).
- ⁴⁶ H. Janovjak, M. Kessler, D. Oesterhelt, H. Gaub, and D. J. Mueller, *EMBO J.* **22** 5220 (2003).

FIGURE CAPTIONS

Fig. 1. Backbone of the native conformation of the human ubiquitin. Terminal N is a methionine and terminal C is a glycine.

Fig. 2. Conformations of ubiquitin stretched by 100 Å. The pulling devices are attached to amino acids indicated on the right hand side. The values of the extension parameter, L are 112.69, 94.67, and 95.68 Å top to bottom respectively.

Fig. 3. Force-extension relationships for a single ubiquitin at $\tilde{T}=0$ (the solid line) and 0.3 (the dotted line). The panels correspond to various force attachments as indicated on the right hand side in each panel.

Fig. 4. Similar to Figure 3 but the force is plotted versus extension.

Fig. 5. Force-extension relationships for a single ubiquitin at $\tilde{T} = 0$ stretched by various residues. The residues to which forces are attached are shown in the right hand corner of each panel.

Fig. 6. The $\tilde{T} = 0$ stretching scenarios of ubiquitin corresponding to pulling by residues that are indicated. The symbols indicate particular types of contacts and the following convention is used: solid circles segments 12-17 and 65-72 interacting with the α helix 23-34; open circles 1-7 with 41-49; open pentagons 1-7 with 12-17, open squares [1-7 and 12-17] with 65-72; solid triangles 41-49 with 65-72; open triangles 41-49 with 41-49; the stars indicate all other contacts.

Fig. 7. The dependence of the maximum force on the logarithm of the pulling speed. The solid symbols and lines are for the N-C stretching. The open symbols and dotted lines are for the Lys48-C mode of stretching. The square, triangle, and circle symbols correspond to $\tilde{T}=0$, 0.2, and 0.3 respectively.

Fig. 8. Force-displacement patterns for a polyubiquitin composed of five repeats at $\tilde{T}=0$ (the solid line) and 0.3 (the dotted line). The panels correspond to various linkages between

the monomers. Force attachments are consistent with the type of linkage. For instance, "48-76" indicates that the molecules are linked so that the C terminal of the first protein is covalently attached to the Lys48 amino acid of the second protein, and so on. The pulling device is attached to the Lys48 amino acid in the first domain and to the C terminal in the fifth domain.

Fig. 9 Force-extension patterns corresponding to Figure 8.

Fig. 10. Conformations of five ubiquitins linked as described in Figure 8 and pulled by 250 Å.

FIGURES

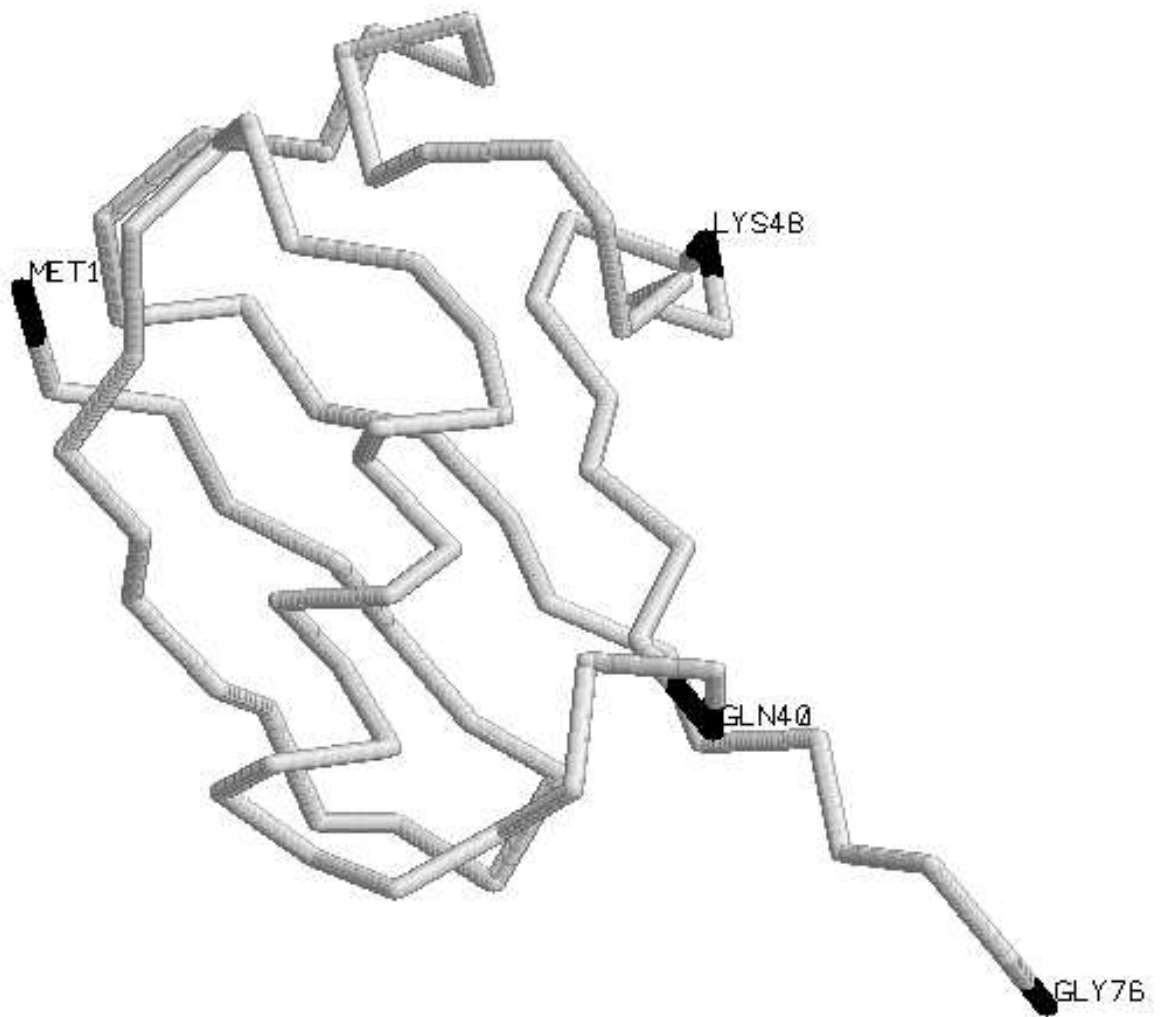


FIG. 1.

1ubq

d=100 Å

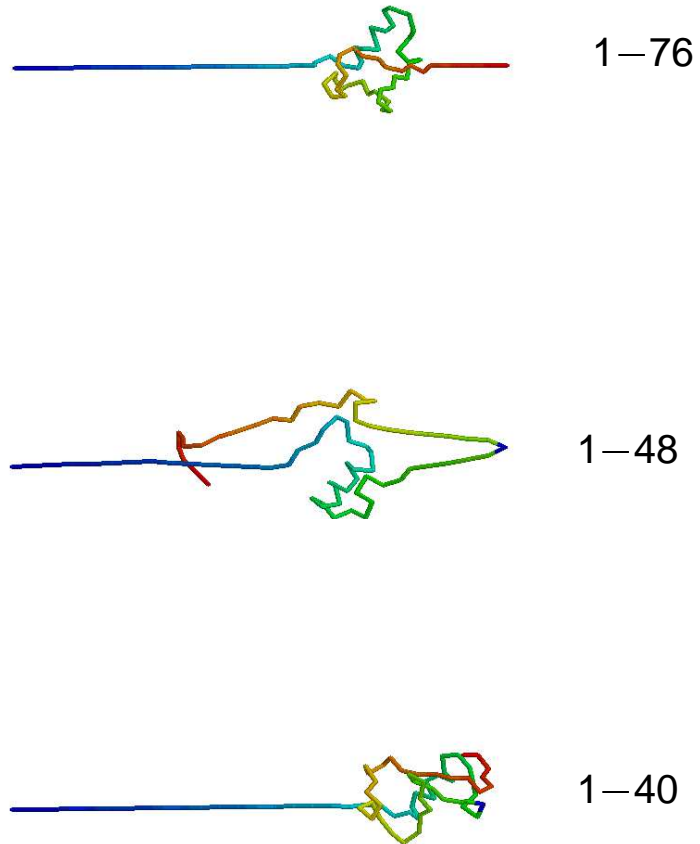


FIG. 2.

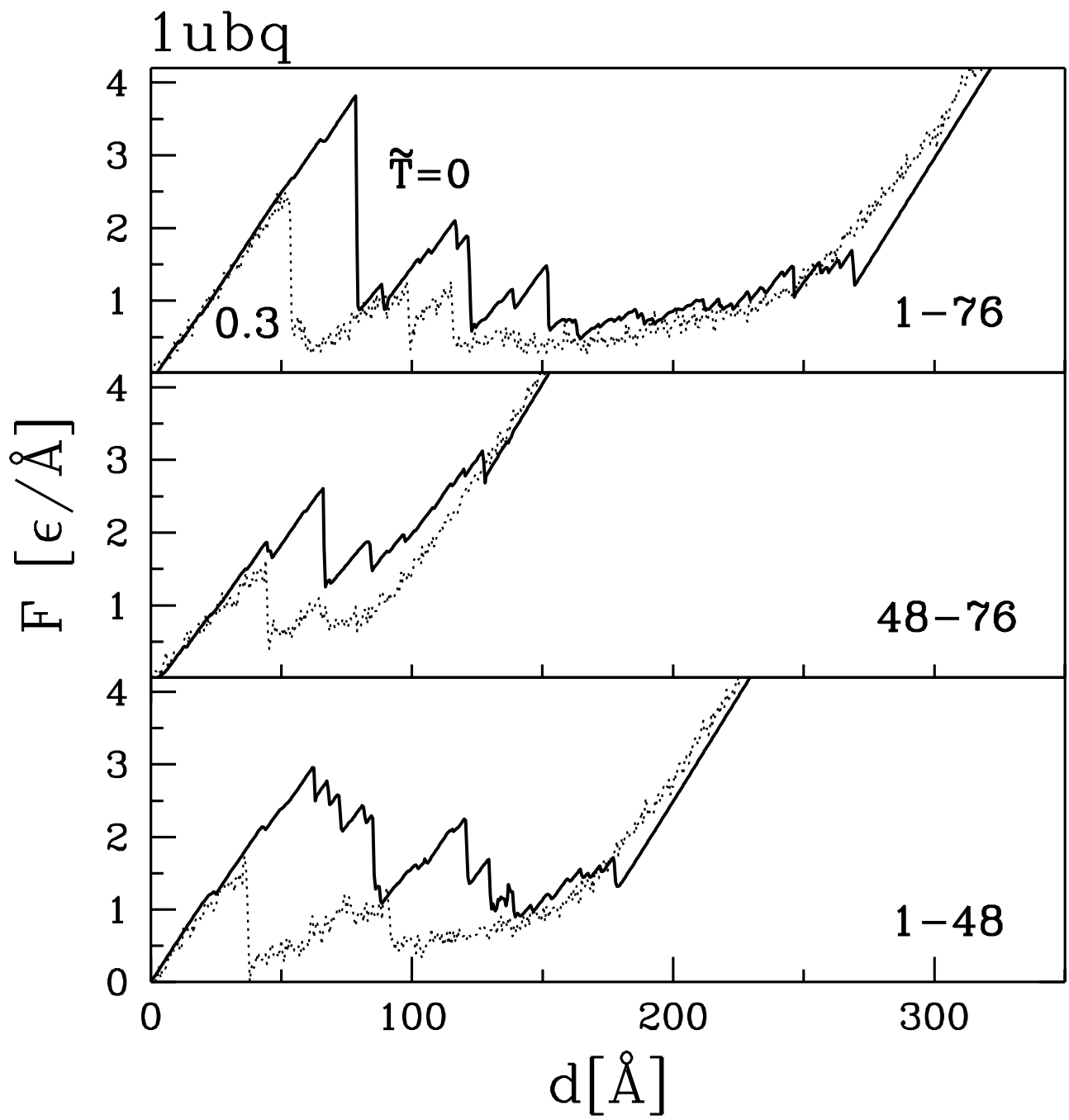


FIG. 3.

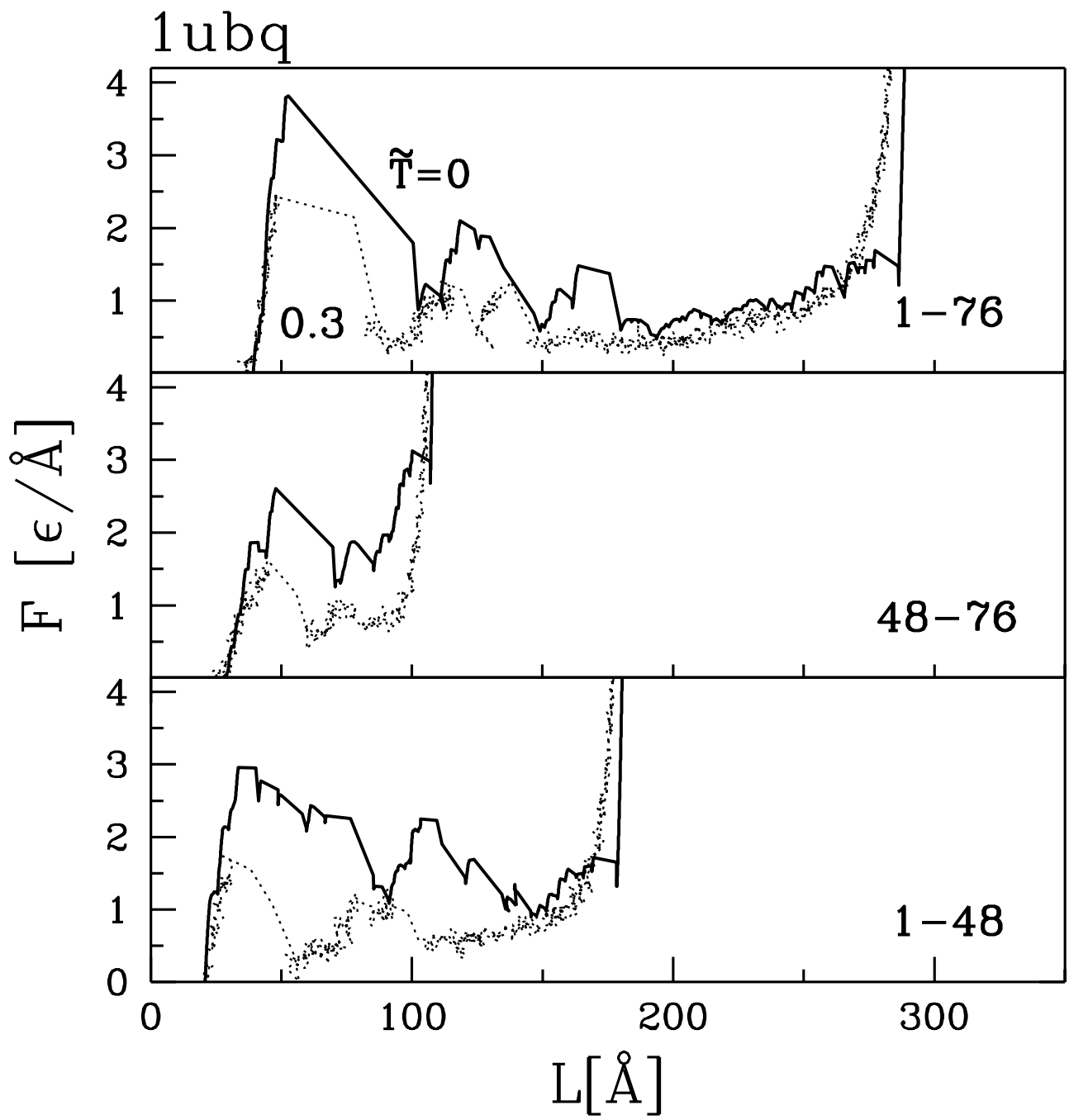


FIG. 4.

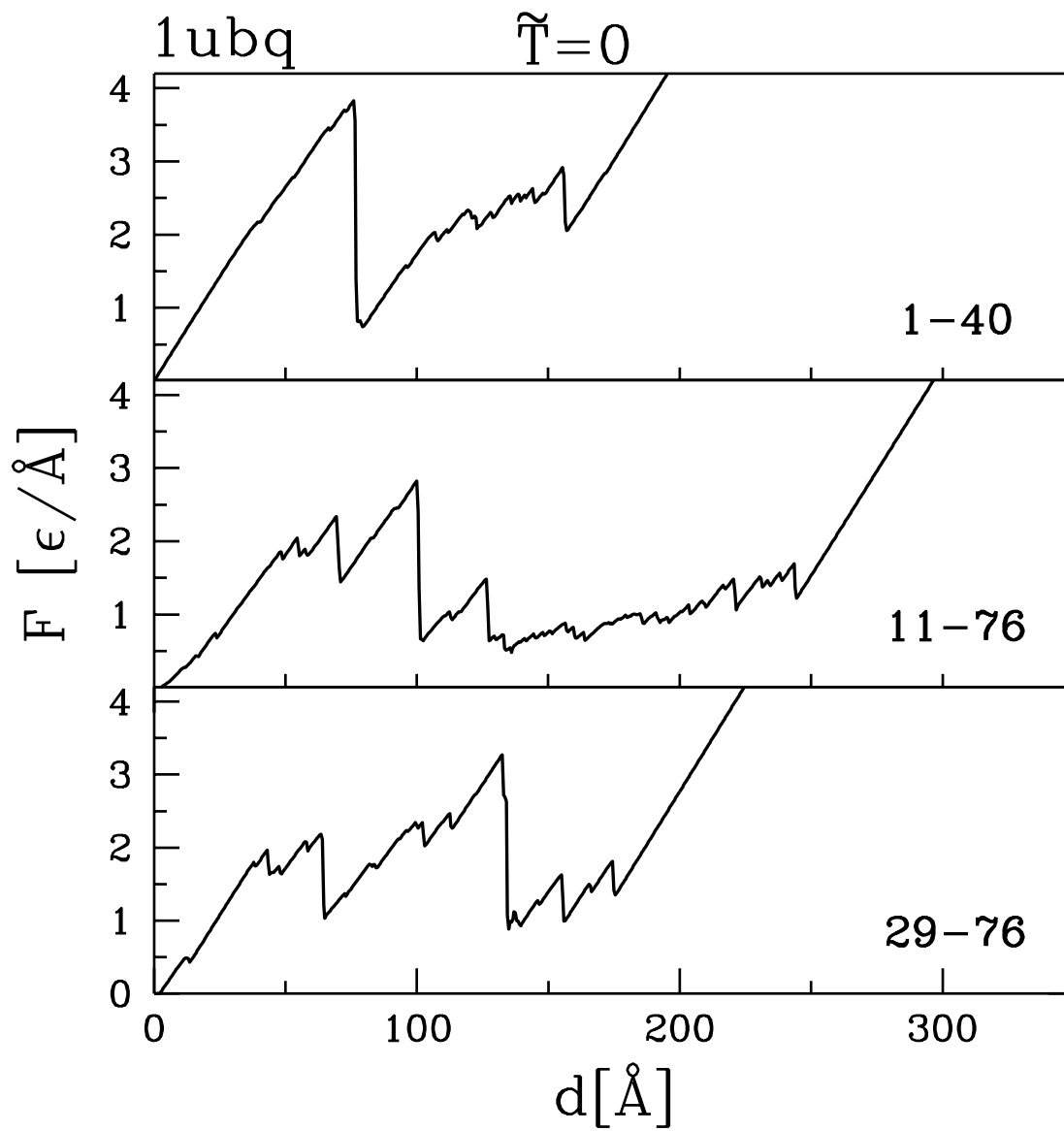


FIG. 5.

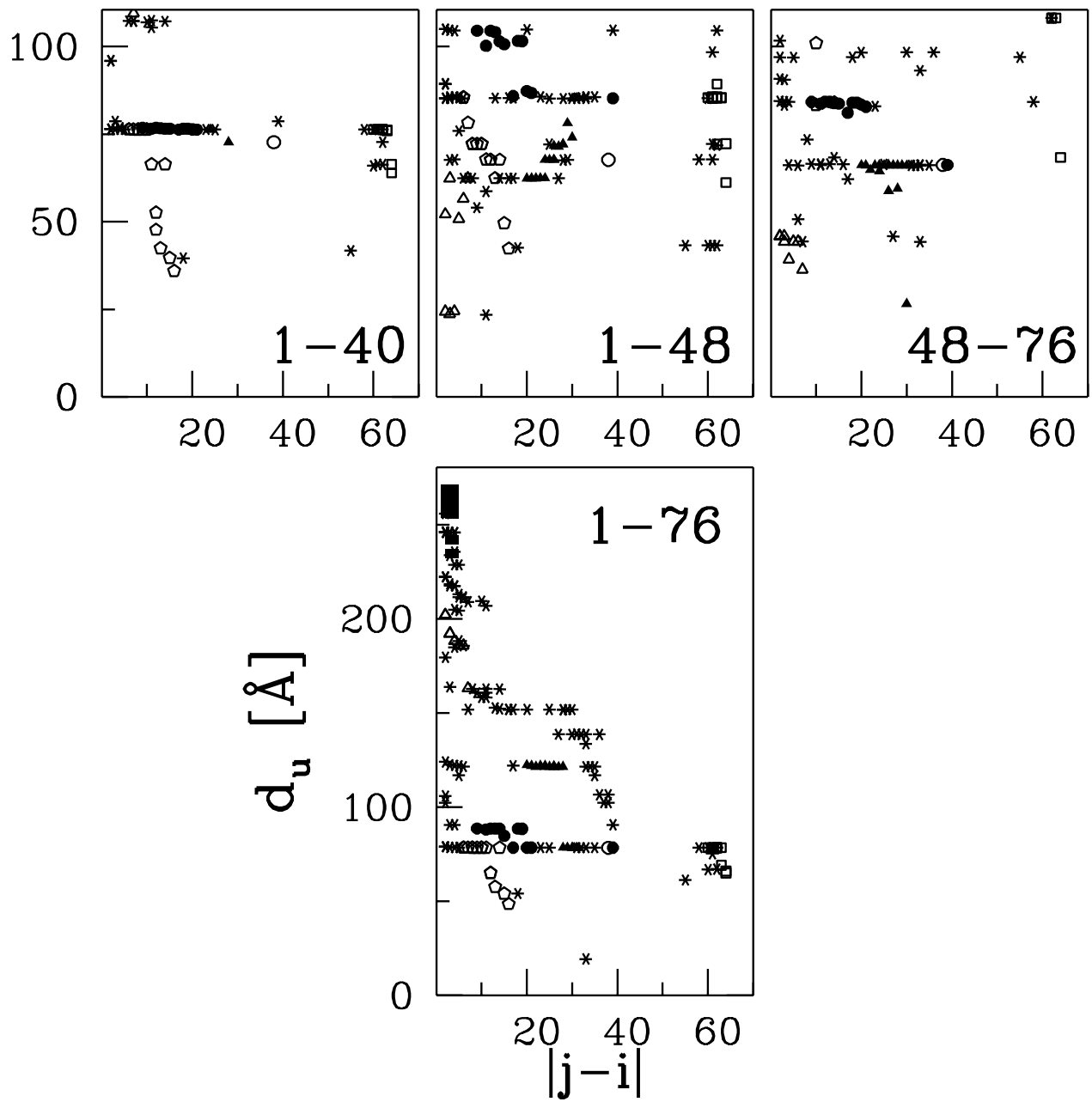


FIG. 6.

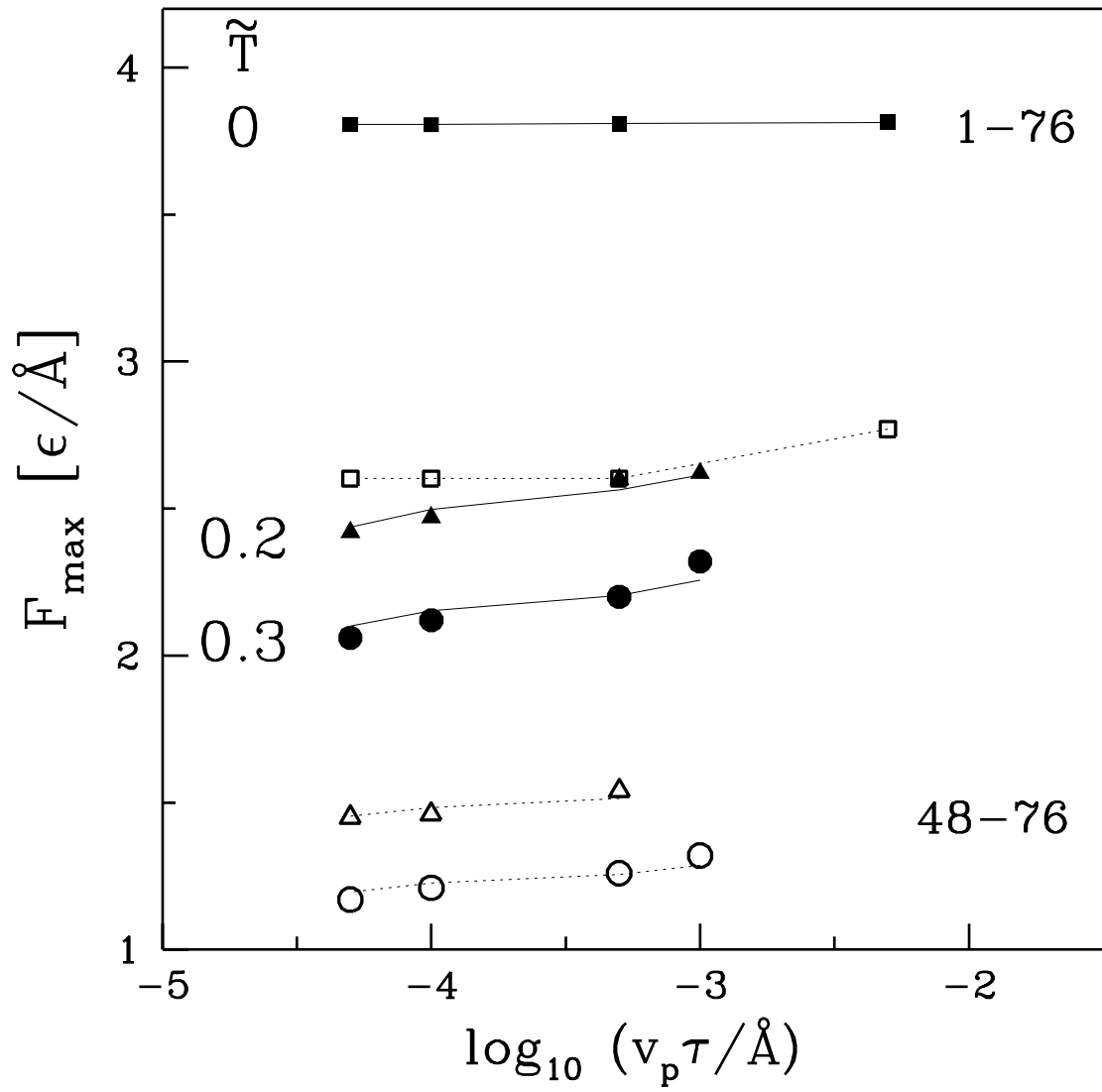


FIG. 7.

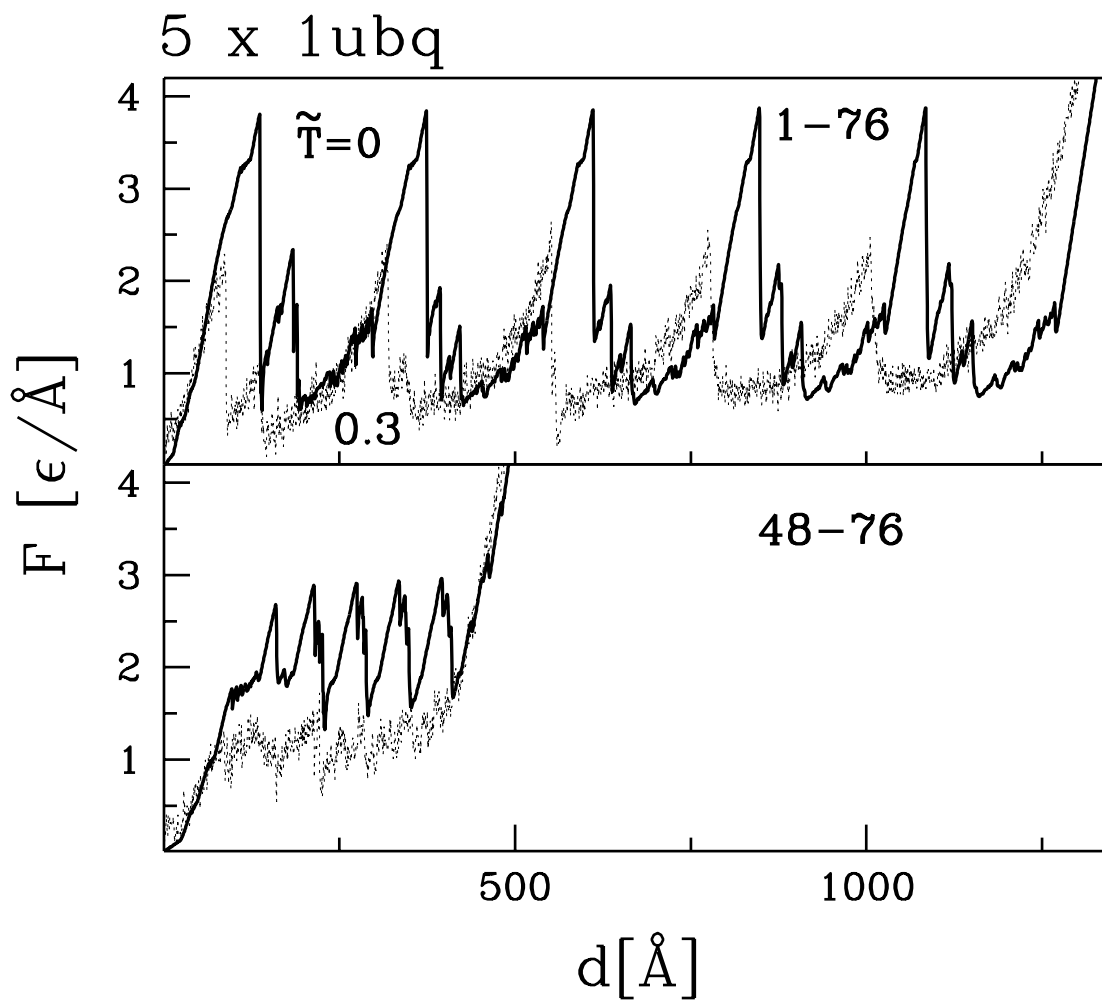


FIG. 8.

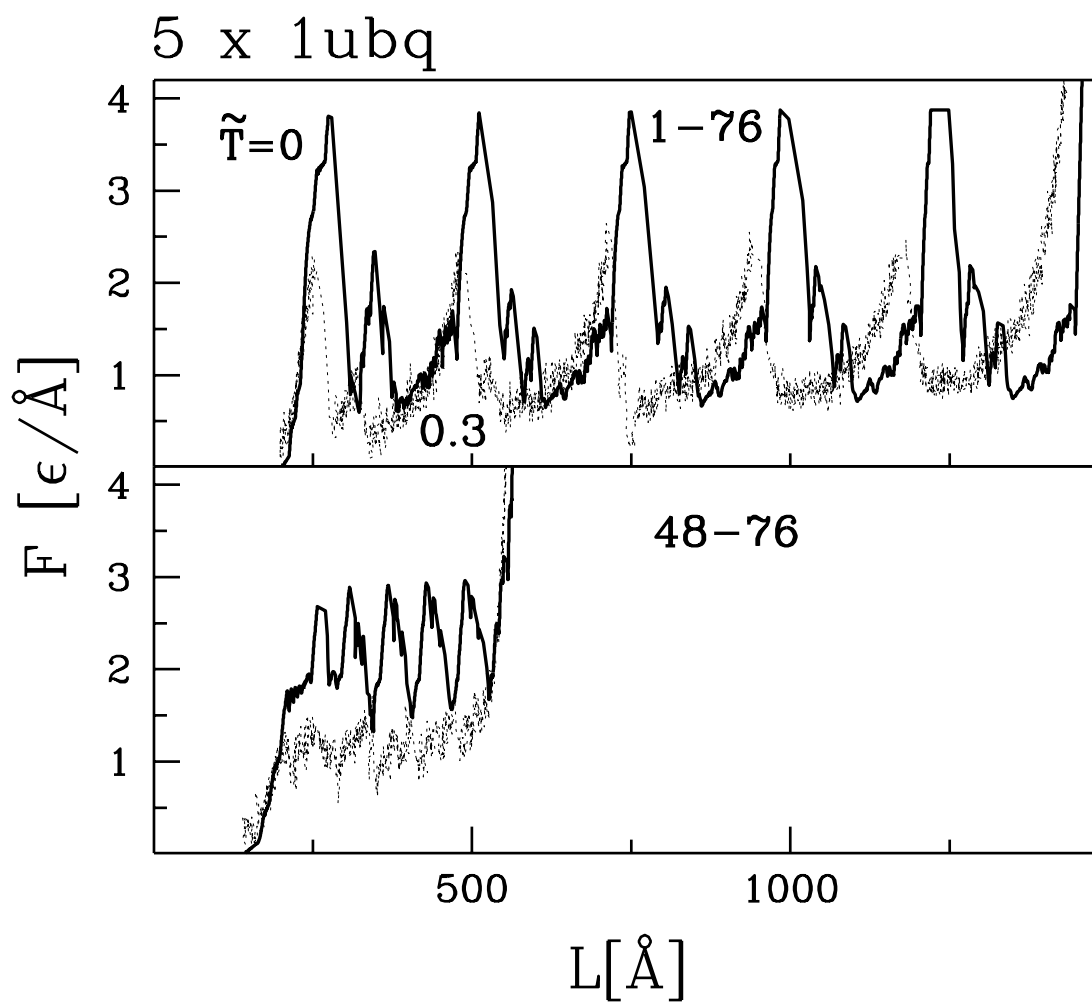


FIG. 9.

$5 \times 1\text{ubq}$

$d=250 \text{ \AA}$



1–76



48–76

FIG. 10.